

Analytical and Numerical Study of an Iron-Core Shunt-Compensation Reactor on a Mixed Transmission Line

N. Pfeifer, M. Kizilcay, P. Malicki

Abstract-- In today's grid reinforcement in Germany, more and more underground cable sections are being installed at the 400-kV level. They are mostly used near cities or to overcome other obstacles. Consequently, mixed transmission lines are formed, which include overhead line and cable sections at this voltage level. Typically, shunt reactors are used on such lines to compensate the capacitive reactive power. In addition to the compensation degree, the type of the reactor is also important. These can be realized as an air core coil or as a coil with iron core. Especially when using iron core coils there are additional effects like saturation or zero-missing effects, which have to be investigated before erecting a mixed transmission line. These effects are numerically simulated and validated and explained using an analytical method. With the aid of a simplified model, the system properties have been investigated and applied to the transmission line.

Keywords: EHV Cable System, EMT, Iron-Core Reactor, Shunt Reactor, Mixed Transmission Line, Zero-Missing Effect

I. INTRODUCTION

To realize the transition from fossil fuel and nuclear power to regenerative power generation, several new transmission lines will be built in Germany. This expansion of the existing transmission grid at 400-kV level, especially in densely populated areas, cannot be realized by overhead lines, as they require much larger space and are not accepted by the population. The possible alternative is underground cables that can be placed in tunnels or protective tubes in the underground within or near urban areas. Consequently, so called "mixed transmission lines" are formed consisting of overhead line sections and cable sections.

Compared to overhead lines, the significantly higher capacitance of EHV cables affects both the reactive power consumption of the line and the frequency response [3]. This is getting worse by the fact that two cables per phase are usually installed in parallel to achieve the same transmission power as an overhead line. When operating such lines, it is common to reduce the capacitive reactive power by using shunt reactors. In addition to the compensation power, the coil position and the topology of the mixed transmission line, the reactor type plays a role especially during system transients, for example due to the switching operation [6,7]. Mostly iron-

cored shunt reactors are used due to the more compact design and the lower field strengths around the environment.

In this paper, special attention is paid to the shunt reactor properties including ferromagnetic characteristics of the fixed and variable iron-core coils with regard to the saturation. Compensation effects will be considered and explained and better understood with an analytical model. The aim is to understand the analytical method and to be able to identify critical conditions in advance with little effort in future investigations.

II. STUDIED SYSTEM

In order to avoid further influences due to the interaction by larger networks, only a small sized mixed transmission system is considered in the context of this work. It is modeled and simulated with the help of EMT. In order to apply an analytical method additionally, the model has been significantly reduced.

A. Description of the EMT-Model

The examined transmission line connects two stations on the 400-kV HVAC level, which are about 19 km apart. As shown in Fig. 1, there is a 10 km cable section within the line. Within this cable section various placement methods are implemented and the cable section can be divided into three major sections in terms of cross-bonding. There are a 3 km long overhead line (OHL) to the left of the cable transfer station (CTS) 1 and a 6 km OHL to the right of the CTS. Those overhead lines end up in the network nodes called station 1 and 2. They are represented by voltage sources behind three-phase positive- and zero-sequence short-circuit impedances. For the same transport capacity of the overhead lines, two cables must be used in parallel, so that a total of 12 XLPE cables with 2500 mm² copper cross section will be installed.

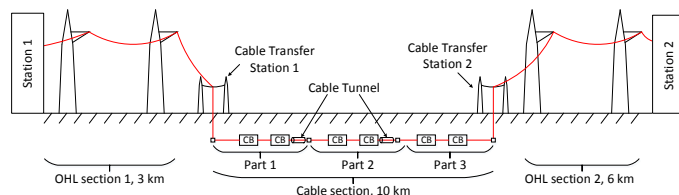


Fig. 1. Overview of the studied system

The three major parts of the cable section have almost the same length. The lengths of the respective cable parts should be approximately the same to allow for optimal cross-bonding

N. Pfeifer, M. Kizilcay and P. Malicki are with the Department of Electrical Engineering and Computer Science of the University of Siegen in Siegen, Germany. (e-mail of corresponding author: nils.pfeifer@uni-siegen.de).

Paper submitted to the International Conference on Power Systems Transients (IPST2023) in Thessaloniki, Greece, June 12-15, 2023.

of the cable sheaths, although the different installation methods make this difficult. The capacitive reactive power of the cable section is to be compensated at the both CTS's. The two OHL sections use the same 400-kV tower type. Only the two circuits are located on this tower to avoid any influence from other voltage levels. The tower geometry is shown in Figure 2. For the simulation in EMT, the *Bergeron* line model is used because a frequency-dependent model such as ULM becomes unstable due to the short distance with many conductors. The parameters are determined for 500 Hz, since preliminary tests have shown that the entire transmission line has the lowest resonant frequency in this frequency range and that both lower and higher frequencies are reproduced with sufficient accuracy.

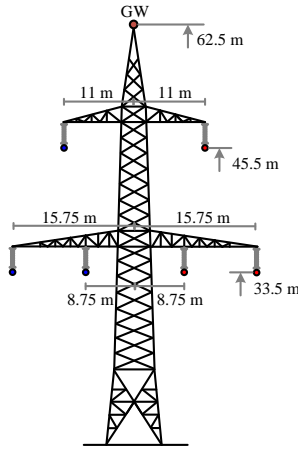


Fig. 2. Tower geometry for a double-circuit 400-kV OHL

Both air core and iron core shunt reactors are to be considered in the investigation. Consequently, two different coil models are used as shown in Fig 3 [4, 6].

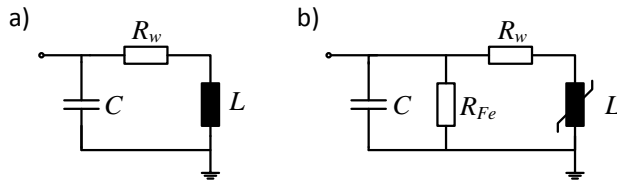


Fig. 3. Compensation model for one air coil (a) and with iron core (b)

A linear inductor can be used for an air core coil (Fig. 3, a). In addition, a resistor for the copper losses of the windings and a capacitor, which represents the capacitance between the windings. In contrast, the coil with iron core is more complicated, because it is modelled by a nonlinear inductance (see Fig. 4). Furthermore, there is an additional parallel resistance to represent iron core losses. The windings are star-connected and can be modeled individually, since the structure of the compensations is very symmetrical and there is no need to model the mutual inductance.

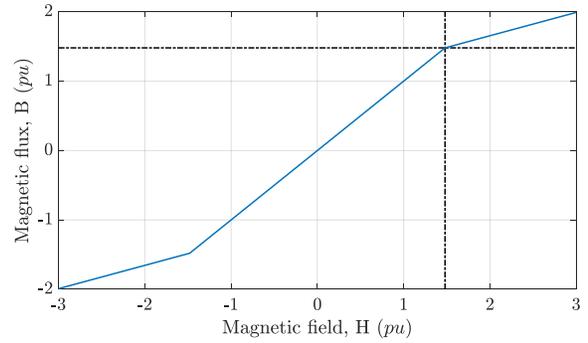


Fig. 4. Saturation characteristic of a fixed compensation reactor in per unit quantities

In the diagram, the saturation is reached at 1.48 pu, which is common for a fixed compensation coil with iron core. For the application with the compensation coil that has on-load tap changer, this must be adapted to the respective stage. The model parameters for the different compensation coils are listed in Table 1.

TABLE I
MODEL PARAMETERS OF THE DIFFERENT TYPES OF COMPENSATION COILS

No.	Reactive Power	Coil Type	L_{lin}	Sat. Threshold	Com. Level
1	150 Mvar	Air, const	3.4 H	---	48 %
2	60 Mvar	Iron, const	8.49 H	148 %	19 %
3	120 Mvar	Iron, const	4.24 H	148 %	38 %
4	75 Mvar	Iron, variable	6.79 H	271 %	24 %
5	157 Mvar	Iron, variable	3.24 H	186 %	50 %
6	250 Mvar	Iron, variable	2.04 H	148 %	79 %

The air coil (No. 1) has no saturation and always behaves linearly. For the fixed iron core coils (No. 2 and 3) and the maximum stage of the variable reactor (No. 6), a saturation threshold of 148 % is assumed, which has been adjusted for the lower power steps for no. 4 and 5.

B. Model reduction for an analytic method

In order to better understand the saturation of the iron core and to make the effects on current and voltage clearer, the transmission line model will be simplified so that it can be described with discrete components. The investigations always consider the open-circuit case, which means that the line inductances can be neglected due to the low current. Consequently, only the line capacitance must be modelled by a capacitor. The behavior of the overhead line can be determined with the help of EMT, where only the positive-sequence conductor-to-earth capacitance is relevant. For the coaxial cables, it corresponds to the conductor-sheath capacitance. The total capacitance of the transmission line in Fig. 1 results in $C_{TM} = 6.27 \mu F$.

The shunt reactor model is also simplified so that only the inductance remains, whereby this is nonlinear for a coil with iron core. The inductance values are listed in Table 1. Putting them together results in the circuit, which is shown in Fig. 5 [1].

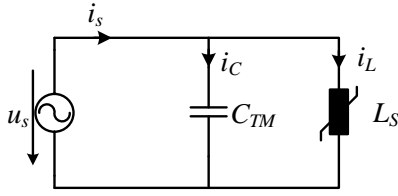


Fig. 5. Simplified model for analytic method

Using this circuit, a node equation can be written for the three branch currents [1]. If only the imaginary part is considered, i_s can be obtained as

$$i_s = i_C + i_L = \frac{u_s}{\omega \cdot L_S(\phi)} - \omega \cdot C_{TM} \cdot u_s \quad (1)$$

The source current is composed of the two partial currents flowing through the capacitance and the inductance. The capacitive part can be represented by a simple straight line in the VI diagram, where the slope depends on frequency and capacitance C_{TM} . The inductance L_S has a dependence on the magnetic flux, which causes saturation of the iron core. Thus, the function for the inductance must first be derived from the characteristic curve in Fig. 4. This must be done for each compensation type. To allow analytical consideration, only the self-inductance is used. The diagram of the equation (1) with the individual components can be seen in Fig. 6.

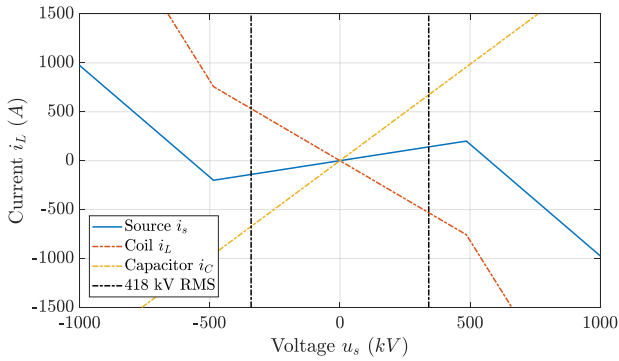


Fig. 6. Representation of the components of equation (1) in a VI diagram

In addition, the magnitude of the normal operation voltage (phase-to-phase, here 418 kV) is marked. It is noticeable that the shunt compensation takes place in the linear range and the source current increases linearly with the voltage. The investigations and simulations always assume a symmetrical three-phase system, consequently only the quantities of *phase a* are considered.

III. CHARACTERISTICS OF IRON-CORED SHUNT COMPENSATIONS

First, the transmission line in normal operation is considered and the relationship between VI diagram and time domain is described. As already mentioned, the transmission line is supplied only at one end and the other end is open. In addition, various parameters such as grid frequency, compensation type, compensation power and length of the line or the line capacitance also have an influence on the system behavior.

For normal operation, a voltage of 418 kV (1.045 pu) is assumed and the system is in steady state. Furthermore, the complete transmission line is considered with a 250-Mvar shunt reactor (No. 6). The time-varying plots of currents in Fig. 7 correspond to the VI diagram in Fig. 6.

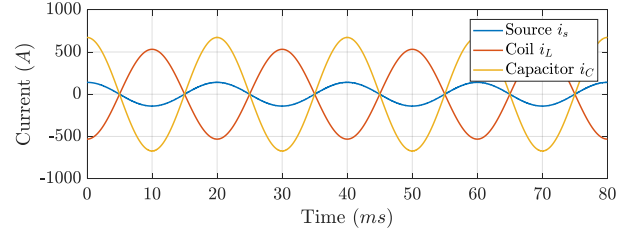


Fig. 7. Time domain simulation of the currents for coil no. 6

It can be seen from the amplitude values that the capacitive current is compensated by the coil current, so that the source current is reduced. This can also be seen in Fig. 6, just as the overall system remains capacitive. Furthermore, there is no distortion because the coil is operated in the linear range.

The VI diagram of the inductive currents for different compensation coils according to Table 1 is shown in Fig. 8.

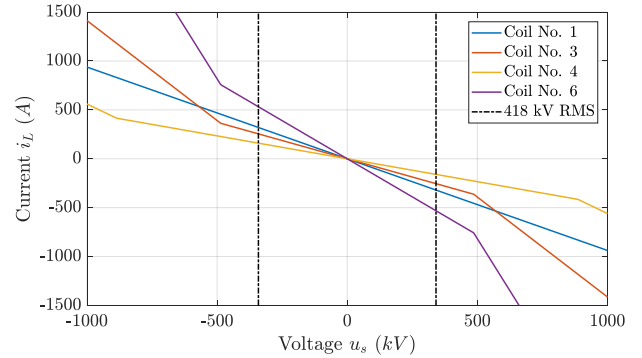


Fig. 8. Coil currents for different compensation cases at 50 Hz

As expected, the gradient determined by the inductance, which is, however, only constant for coil no. 1 (linear, air-core coil) over the entire voltage range. The gradients of coils no. 3 and no. 6 are different, but the saturation voltage threshold is identical. Due to the variable step of power level of coil no. 4, the saturation voltage shifts significantly upwards. From the previous study using equation (1) and Fig. 6, it is clear that the coils can saturate due to an overvoltage, which can occur as a result of a switching operation, for example. For the investigation of overvoltages, a voltage increase to a constant value with a constant grid frequency is assumed, so that the time domain plots can be traced by the corresponding VI diagram. For this purpose, the source currents for certain compensation types and addition marks for the source voltage are shown in Fig. 9.

Higher system voltage values are chosen to operate the coils at the limit of their linear range (595 kV , 1.423 pu) and in the saturation region (702 kV , 1.679 pu). In the case of coil no. 5, the saturation voltage is even higher since the coil is equipped with an on-load tap changer to adjust the compensation level.

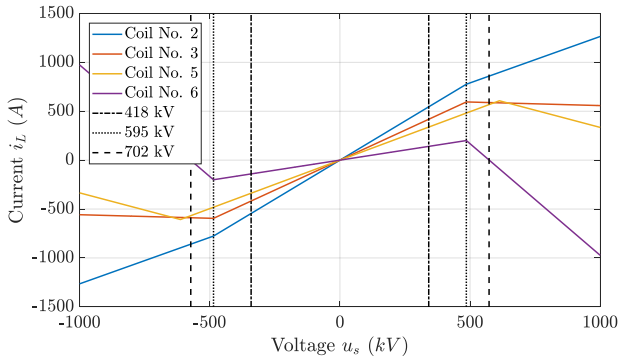


Fig. 9. VI diagram of the source current for different types of coils with additional voltage markers at power frequency 50 Hz

The coil no. 3 enters into the saturation region above 595 kV (1.423 pu), but the current remains almost constant. Coil no. 6 provides overcompensation in the saturation region, which is why the current decreases again above 595 kV (1.423 pu). This is also shown in the time domain simulation in Fig. 10.

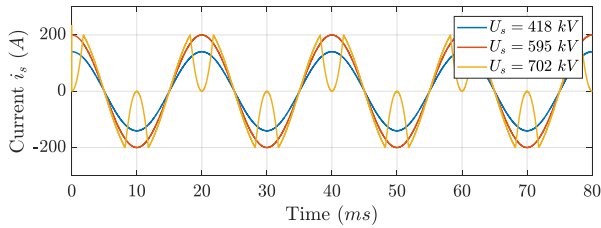


Fig. 10. Time domain simulation of the source current for coil no. 6 for different source voltages

At voltage up to 595 kV (1.423 pu) the amplitude behaves linear and the current remains sinusoidal. By increasing the voltage to 702 kV (1.679 pu), the current decreases abruptly until it touches the zero line again, which is also noticeable in the VI diagram in Fig. 9. The current of coil no. 3 in Fig. 11 shows a similar and less distorted behavior.

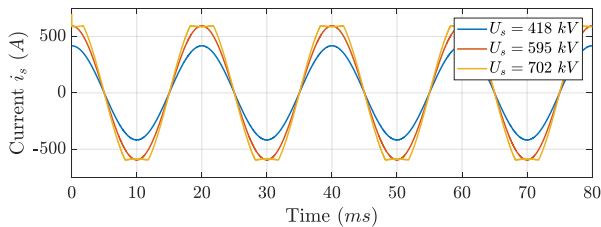


Fig. 11. Time domain simulation of the source current for coil no. 3 for different source voltages

Since the coil no. 3 has a VI characteristics with almost constant current in the saturation region above ± 595 kV (1.423 pu), the current in the time domain is distorted such that it remains at a constant level for a while during the saturation phase, which can be seen in the spectrum in Fig. 12.

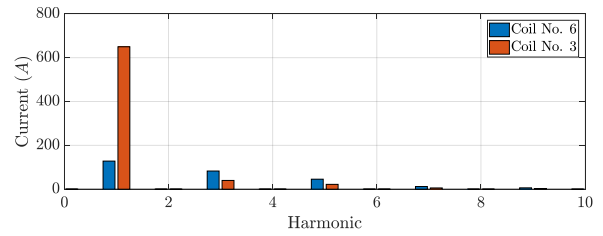


Fig. 12. Spectrum of the source current of the coil no. 3 and no. 6 for the source voltage of 702 kV RMS

First of all, the 50-Hz amplitudes are clearly larger with the smaller compensation power (coil no. 3). However, in both cases further oscillations are added, which are caused by the distortion. In the case of coil no. 6, for example, the current reversal triples the frequency, which forces the 3rd harmonic. Higher frequencies also occur because the reversal happens abruptly. The spectrum of the source current behaves similarly with coil no. 3. In this case, a square-shape wave signal is generated. That results in the typical spectrum shown in Fig. 12.

Another parameter, which can lead to coil saturation as shown in equation (1), is the frequency. The frequency may deviate from 50 Hz in the case, when the line is deenergized and both circuit breakers are open, so that an oscillation occurs between the compensation and the line. Fig. 13 shows as an example the VI diagram of the coils for 30 Hz.

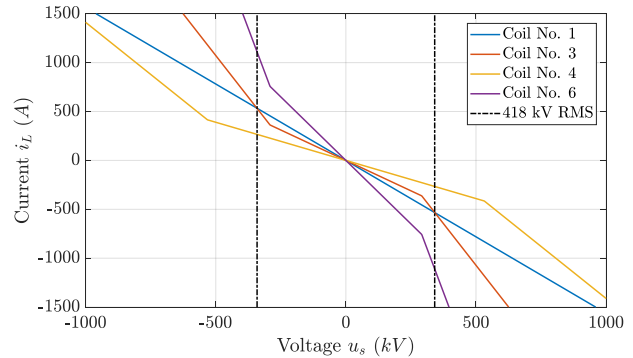


Fig. 13. VI diagrams of the coils currents for different compensation cases at 30 Hz

Due to the changed frequency, the gradients of all types increase so that saturation is reached earlier with regard to voltage. Consequently, saturation occurs in coils no. 3 and no. 6 within the normal operating voltage range. The saturation can also be observed in the VI diagrams of the source current in Fig. 14.

The capacitive current is also affected by the frequency, so the two cases are clearly different. Coil no. 6 overcompensates for the capacitive current, which is amplified in the saturation region.

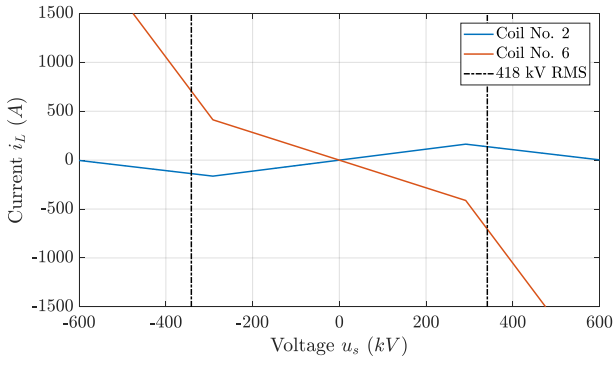


Fig. 14. VI diagrams of the source current at 30 Hz for the coils no. 2 and no. 6

In the case of coil no. 2, on the other hand, overcompensation only occurs in the saturation, so that a reversal of current takes place at the threshold of the saturation voltage. All properties also show up in the time domain simulation in Fig. 15.

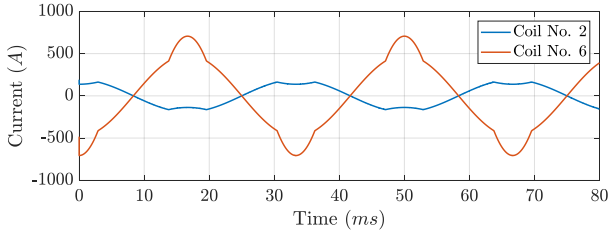


Fig. 15. Source currents for the coils no. 2 and no. 6 for a 30-Hz source voltage of 418 kV RMS

It is immediately noticeable that both plots are opposite, since the case with the coil no. 2 shows a capacitive and the case with the coil no. 6 an inductive behavior. While coil no. 6 causes an increase of the current peak, which is expected for a saturation, the opposite behavior happens in the case of coil no. 2 (see Fig. 15). It results in that the peak of the sinusoidal shape is cut off and reversed.

Basically, operation of compensations at other frequencies is not realistic. However, free oscillations at lower frequencies can occur between the transmission line and shunt reactor when the line is switched off. For the system with coil no. 2, this would result in a frequency of 21.82 Hz, which would cause saturation of the shunt reactor.

IV. SATURATION CAUSED BY ENERGIZING IN THE VOLTAGE ZERO-CROSSING

Based on the previously considered properties, it can be now attempted to consider the energizing of the transmission line at the voltage zero crossing. The far end of the transmission line is still open. Equation (1) is considered again, but it must be adapted so that it describes the behavior after energization. Basically, an adjustment is only necessary for the inductance, since an offset results from the integration of the voltage in the time domain due to the switching at the voltage zero crossing. This offset must be included in the saturation characteristic curve, since the magnetic flux in this

configuration depends directly on the voltage.

$$i_s = i_C + i_L = \frac{u_s}{\omega \cdot L_s(\phi(u_s + u_0))} - \omega \cdot C_{TM} \cdot u_s \quad (2)$$

The voltage u_0 depends on the energizing moment and is exactly the amplitude of the source voltage when energizing at the voltage zero crossing. This will preload the iron core, which leads to a displacement as shown in Fig. 16.

In the VI diagram, the zero point is shifted to the negative amplitude of the operation voltage, so that this voltage is present at the beginning and no current is flowing yet. After energizing the coil current moves only in the negative range and in the model no losses are considered, it also comes to no adjustment of the offset.

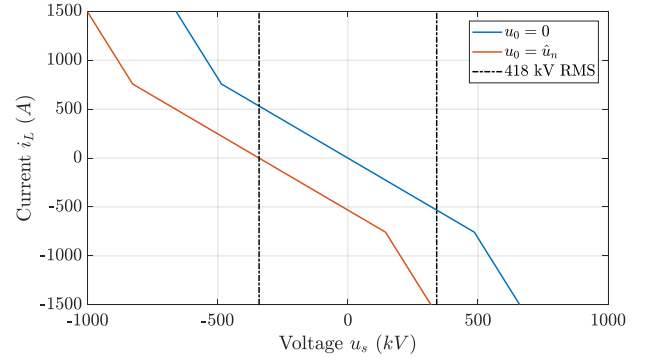


Fig. 16. Shift of the coil current of coil no. 6 when energizing at voltage zero crossing

The current through the capacitor or the path is not affected by the moment of closing, which is why no adjustment is necessary in the term of the capacitive current in equation (1) and the curves remain unchanged. In the source current only the inductive part is influenced, which results in the VI diagrams in Fig. 17.

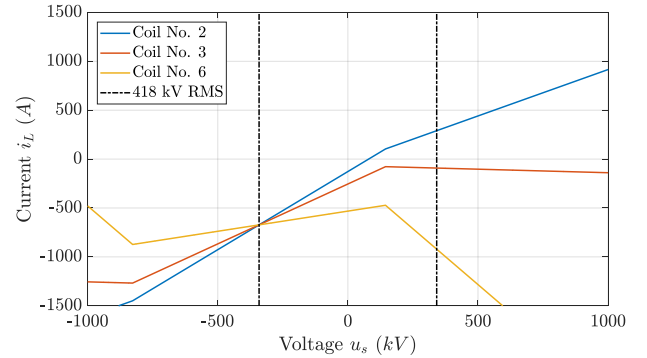


Fig. 17. Source current for different coils when energizing at voltage zero crossing

With the smallest compensation power by the coil no. 2, there is still a zero crossing of the current within the range of the normal operation voltage. However, the saturation voltage shifts so that it is also within the range of the operation voltage and distorts the source current. The other two coils also reach saturation within the operating voltage. For those, there is the additional problem that there is no zero crossing of the current. This is also shown in the plots in the time domain (see Fig. 18).

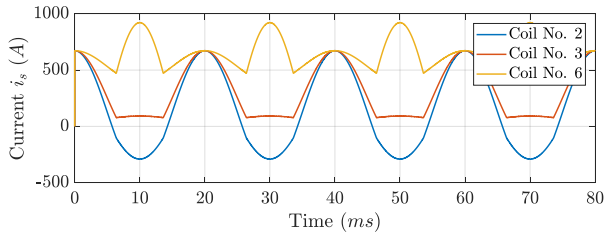


Fig. 18. Source current in the time domain for different coils when energizing at voltage zero crossing

The energization occurs at $t = 0$ ms. In all plots in Fig. 18 there are no additional high-frequency oscillations, because the model components are modelled with bundled devices and are simulated only for 50 Hz. The source current with the coil no. 2 in operation is distorted due to the saturation, but the sinusoidal form is almost preserved. Referring to the VI diagrams in Fig. 17, the current zero crossings after energization are missing in the other two cases with the coils no. 3 and 6. Furthermore, the other two coils show similar saturation behavior as in the previous chapter, where the saturation was caused by an overvoltage. Coil no. 3 shows a constant current for a short duration in a period and coil no. 6 shows a current reversal, but here the saturation only occurs in the positive current region as shown in Fig. 18.

V. COMPARISON WITH THE FULL MODEL

In this chapter, the results obtained with the simplified model will be transferred to the more complex and detailed model of the transmission line. For this purpose, the normal operation with one open line end, which was considered in section III, will be compared first. The simplified model is described by the analytical method, while the detailed model in EMT is calculated numerically with more accurate component properties such as losses. For the normal source voltage of 418 kV and the coil no. 6, the plots in the time domain are shown in Fig. 19.

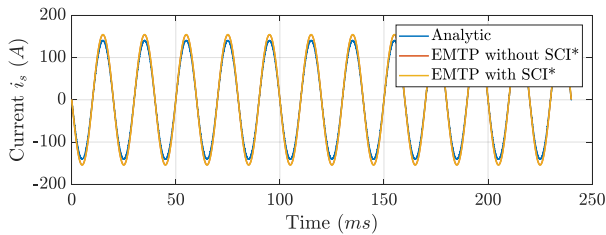


Fig. 19. Comparison between the simplified and the detailed model in normal operation for coil no. 6 with and without main short-circuit impedance (SCI*).

For the detailed model in EMT, a further differentiation is made. The three-phase short circuit impedance (SCI) of the source network, will be removed once from the model and added to the model once. However, it turns out that this has no significant influence in steady state. Since no longitudinal inductances and also no length could be taken into account in the simplified model, the currents in the more accurate EMT models are somehow higher. Because no equipment is overloaded in normal steady-state operation, the entire system behaves linearly, which is why there are no additional

distortions. More interesting is the saturation of the shunt reactors due to an overvoltage as shown in Fig. 20.

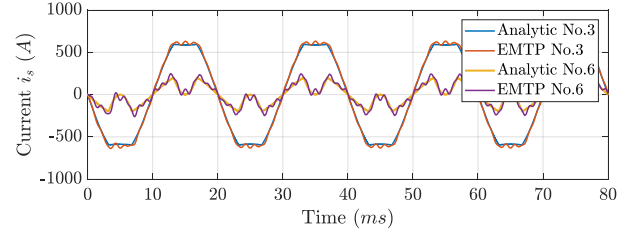


Fig. 20. Comparison of the source currents by the simplified and the detailed model in normal operation at 702 kV without SCI

The Fig. 20 shows cases with the coil no. 3 and no. 6. Both are in saturation due to the operating voltage of 702 kV. The basic current shapes between the cases match well. In the detailed model further oscillations are expected, which are caused by the more accurate line model and are initiated by the saturation of the shunt reactor. The additional oscillations remain permanently, because they are triggered by the saturation in each period. When the line is energized, the oscillating behavior of the line is forced much more strongly, which is shown in Fig. 21.

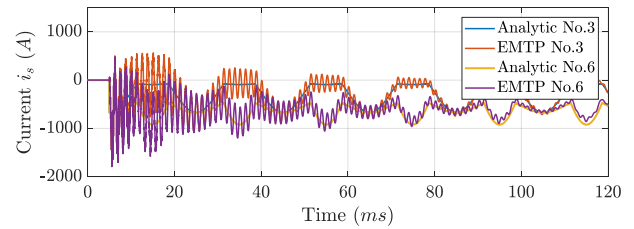


Fig. 21. Comparison of the source currents by the simplified and the detailed model, when energizing the transmission line without SCI at 418 kV

The comparison again shows that the plots are very similar in basic shape, but in this case the oscillations are much more pronounced, making the comparison more difficult. After the higher frequency oscillations have subsided somewhat, it becomes apparent that the basic characteristics are very similar. It is noticeable that the DC offset decreases in the detailed model due to the line losses, while it remains constant, when the simplified model is used. In the previous Chapter IV, it was shown that for both types of coils the current zero crossings are missing which is critical. However, with the detailed model there are initially high-frequency oscillations, so that current zero crossings occur. The coil current was also examined and compared between the two models. The time-varying curves of the coil current are almost identical, so that the plots are not shown here.

VI. CONCLUSIONS

In this paper, a mixed transmission line with overhead line and cable sections and shunt reactors has been studied by means of simulations. Different shunt reactor types with various reactive power levels have been considered and evaluated. In order to be able to deal in particular with the saturation properties of the coils with iron cores, a significantly simplified model was created, which can be described analytically and the model can be represented by

VI diagrams. With the help of this model, different operating conditions and possibilities of saturation were considered. By adapting the model, it was also possible to consider the system behavior after the energization. Finally, the results of various compensation cases analyzed by the simplified model have been compared with the detailed model in EMT and validated.

In principle, saturation does not occur during normal operation of the transmission line since the saturation threshold voltage is significantly higher than the normal operation voltage and a change in the normal grid frequency is excluded. The missing of current zero crossings could also be investigated by both model variants, although the initial transition period cannot be prescribed in the simplified model because the losses in the system and additional oscillations due to the transmission line are not taken into consideration in the simplified model. Through the comparisons it was shown that the simplified model for 50 Hz gives good results.

A special phenomenon arises when switching off the line, which has not yet been investigated in detail, but it results in an oscillating frequency deviating from 50 Hz. After disconnecting the transmission line, it oscillates with the shunt reactor at a lower frequency than 50 Hz at compensation levels below 100 % and the saturation of the shunt reactor is thus reached earlier.

All effects could be validated and justified with the analytical model, so it is advisable to use it in future investigations as well. Both the saturation effects and the shapes of the currents, even at different moments of energizing, can be easily described by the analytical method. For more complex transmission lines with several different compensations or other operating conditions, the analytic method can be extended.

VII. REFERENCES

- [1] "Resonance and Ferroresonance in Power Networks", Working Group C4.307, CIGRE Technical Brochure 569, February 2014.
- [2] H. Khalilnezhad, S. Chen, M. Popov, J.A. Bos, J.P.W. de Jong and L. van der Sluis, "Shunt Compensation Design of EHV Double-Circuit Mixed OHL-Cable Connections", ET International Conference on Resilience of Transmission and Distribution Networks (RTDN) 2015, 2015
- [3] "Power System Technical Performance Issues related to the Application of Long HVAC", Working Group C4.502, CIGRE Technical Brochure 556, October 2013.
- [4] M. Kizilcay, K. Teichmann, S. Papenheim and P. Malicki, "Analysis of Switching Transients of an EHV Transmission Line Consisting of Mixed Power Cable and Overhead Line Sections", International Conference on Power Systems Transients (IPST 2017), Seoul, 2017
- [5] A. Mackow, M. Kizilcay, "Transient Studies of Power Cable Sections in a 380-kV Transmission System", 9th International Conference on Insulated Power Cables, Versailles, France, 2015
- [6] N. Pfeifer, M. Kizilcay and P. Malicki, "Evaluation of different Reactive Power Compensation Types of a Mixed 400-kV Transmission Line with an Automated Simulation in EMTP-ATP", European EMTP-ATP Conference 2022, Mannheim, Germany, 2022
- [7] N. Pfeifer, M. Kizilcay and P. Malicki, "Characteristics of a mixed 100-km EHV transmission line with shunt compensation for various topologies", UPEC 2022, Istanbul, Turkey, 2022